AE-388

UDC 539.125.5.164.078:
539.171.02

AE-388

Cross Sections for High-Energy Gamma Transitions from MeV Neutron Capture in ^{206}Pb

I. Bergqvist, B. Lundberg and L. Nilsson

AKTIEBOLAGET ATOMENERGI

STUDSVIK, NYKÖPING, SWEDEN 1970

CROSS SECTIONS FOR HIGH-ENERGY GAMMA TRANSITIONS FROM MeV NEUTRON CAPTURE IN ^{206}Pb

I. Bergqvist* and B. Lundberg

Research Institute of National Defence, Stockholm, Sweden

and

L. Nilsson

AB Atomenergi, Studsvik, Nyköping, Sweden

ABSTRACT

Gamma-ray spectra from neutron capture in ^{206}Pb (radiogenic lead) in the energy range 1.5 to 8.5 MeV were recorded using time-of-flight techniques. The spectrometer was a NaI (TI) crystal, 20.8 cm long and 22.6 cm in diameter. The spectra are dominated by gamma transitions to levels with large single-particle strength, in agreement with predictions of semi-direct capture theories. The theories predict enhancements of the direct capture cross section by a factor of 10 - 15 in the region of the giant dipole resonance. The observed enhancement is about 50.

* Present address: Department of Physics, University of Lund, Lund, Sweden.

LIST OF CONTENTS

INTRODUCTION

A semi-direct reaction process was proposed some years ago by Brown[1], Clement et al.[2] and Lushnikov and Zaretsky[3] to explain the results of nucleon capture experiments in the MeV region. The capture cross sections for heavy nuclei are much larger than can be accounted for by either the compound-nucleus or the direct reaction theories as discussed in connection with experiments by Daly et al.[4], Csikai et al.[5] and Menlove et al.[6].

The gamma-ray spectra following MeV neutron capture show strong intensity of high-energy gamma transitions to low-lying levels with large single-particle strength. Experiments have been carried out by Cvelbar et al.[7-9] and Dinter[10] using 14 MeV neutrons and by Bergqvist et al.[11-13] with neutrons in the range 1.0 to 8.5 MeV. Similar proton capture experiments have recently been performed by Halpern and collaborators[14]. The results show qualitatively the same features as the (n, γ) experiments, i.e. strong gamma transitions to low-lying single-particle levels.

In the semi-direct theory the nucleon capture is suggested to proceed via an intermediate stage involving the excitation of the giant electric dipole resonance. The cross section enhancement is due to the collective nature of this excitation. The intermediate excitation of the giant dipole resonance favours gamma deexcitation directly to low-lying levels, in qualitative agreement with experimental results.

In the present paper, cross sections for ^{206}Pb (n, γ) transitions to individual single-particle states in ^{207}Pb are given as functions of the incident neutron energy. The cross sections are compared with predictions from the direct and semi-direct capture theories. The shapes of the gamma-ray spectra are compared with those expected from the semi-direct reaction process.

EXPERIMENT

Since most of the experimental details have been described elsewhere[12, 13], only a brief outline of the experiment will be given here. The measurements were carried out at the 5.5 MeV van de Graaff accelerator at Studsvik using time-of-flight techniques and a large NaI (TI) detector, 22.6 cm in diameter and 20.8 cm long, placed at 90^{o} to the incident ion beam. A 4096-channel analyser was used in two-parameter mode with flight time recorded in 16 channels and gamma-ray pulse height in 256 channels. The ^{206}Pb sample consisted of radiogenic lead (0.085% ^{204}Pb, 88.38% ^{206}Pb, 8.57% ^{207}Pb and 2.97% ^{208}Pb).

Two series of measurements were performed. In the first series the sample-to-detector distance was 0.9 m and the gamma transition to the ground state in ^{207}Pb was studied. A bismuth sample of the same size as the ^{206}Pb sample was used to determine the background[13]. The neutron binding energy in ^{207}Pb exceeds the ^{210}Bi value by more than 2 MeV (see Fig. 1) whereas the scattering properties of the two samples should be about the same. For other final levels this background could not be used since pulse pile-up effects become troublesome. In the second series of measurements the sample-to-detector distance was increased to 1.4 m and the background was obtained from time channels surrounding the (n, γ) peak in the time spectrum (see Fig. 1, insert figure). In this series gamma transitions to levels up to about 2.7 MeV in ^{207}Pb were investigated.

Neutrons in the energy range 4.5 to 8.5 MeV were produced by the ^{2}H(d, n) ^{3}He reaction in a gas target and below 4.5 MeV by the ^{3}H(p, n)^{3}He reaction. A tritium gas target was used in the first series of measurements and an absorbed target in the second. The neutron yield from the target was monitored by time-of-flight techniques using a plastic scintillation detector placed at 140° to the incident ion beam. This monitor was calibrated against a polythene counter of Los Alamos design[15]. For neutron energies at which the time-of-flight monitor could not be used (i.e. for $E_n < 1$ MeV at 140° corresponding to $E_n < 4$ MeV at 0°) the product of integrated target current, target gas pressure and neutron production cross section was used to normalize to the neutron yield at higher energies.

The pulse-height spectra were unfolded by means of the detector response functions which were determined as described in ref. [12]. In Fig. 2 the response function at 12.77 MeV is compared with the pulse-height distribution obtained from the $^{12}C(n,\gamma)^{13}C$ reaction at the neutron energy 8.50 MeV.

The high-energy parts of the gamma-ray spectra recorded at the neutron energies 5.38, 6.46, 7.46 and 8.43 MeV are plotted in Fig. 3. The results of unfolding the spectra are also shown. The unresolved structure of gamma-rays to levels below 2 MeV was difficult to unfold. However, the intensity to the ground state could be determined within an estimated uncertainty of 20 %. Similar difficulties were encountered in the unfolding of gamma rays to levels between 2 and 5 MeV. The intensity of gamma rays to $E_f = 2.7$ MeV was determined within a relative uncertainty of 20 % for $E_n > 6$ MeV. The structure between $E_f = 2$ and 5 MeV weakens with decreasing neutron energy and only an upper limit of the intensity to $E_f = 2.7$ MeV could be determined for $E_n < 6$ MeV.

Cross sections were evaluated for gamma transitions to the ground state ($p_{1/2}$), to the 0.57($f_{5/2}^{-1}$) and 0.90 MeV ($p_{3/2}^{-1}$) levels and to the 2.74 MeV ($g_{9/2}$) level. The relative intensities to the 0.57 and 0.90 MeV levels are very uncertain and the cross section for the sum of the two transitions was calculated. The results are corrected for neutron and gamma-ray attenuation and for neutron multiple scattering. The method was applied to determine the cross section for production of 4.43 MeV gamma-rays from the $^{12}C(n, n'\gamma)^{12}C$ reaction at 5.43, 6.50, 7.51 and 8.50 MeV. The cross sections were found to be in agreement with the results of Hall and Bonner[16)] and Condé et al.[17)].

RESULTS

Semi-direct capture[1-3)] through the dipole states of nuclei is important in the region of energies near the giant dipole resonance. For Pb the peak of the resonance is at 13.5 MeV and the width about 3.5 MeV. It was possible to produce monoenergetic neutrons of energies up to 8.5 MeV in the present work. The neutron binding energy in ^{207}Pb is 6.74 MeV, which implies excitation energies up to 15.2 MeV, i.e. well above the peak of the giant resonance built on the ground state ($p_{1/2}$). The $g_{9/2}$ state, which is the lowest neutron orbital in the next main shell, is bound by about 4 MeV and the energy available is sufficient to investigate the region up to 1 MeV below the resonance peak.

One way of studying the validity of the semi-direct capture models is to compare the shape of the expected spectrum with the experimental one. Such a comparison is shown in Fig. 4 at the neutron energy 7.46 MeV. The theoretical spectra were obtained from calculations of $^{206}Pb(n, \gamma)$ cross sections using the semi-direct models of Brown[1)] and Clement et al.[2)]. Details of these calculations are given in ref.[12)]. The scattering wave functions were determined using the optical model parameters of Rosen et al.[18)]. Cross sections were evaluated for the $p_{1/2}$, $g_{9/2}$, $i_{11/2}$, $j_{15/2}$ and $d_{5/2}$ single-particle states in ^{207}Pb. The $f_{5/2}^{-1}$ and $p_{3/2}^{-1}$ states at 0.57 and 0.90 MeV are also of importance, since the ground state of ^{206}Pb is not a pure $p_{1/2}^{-2}$ configuration. In the calculations the configuration[19)]

$$\Psi(^{206}\mathrm{Pb}) = 0.65\, p_{1/2}^{-2} + 0.25 f_{5/2}^{-2} + 0.20 p_{3/2}^{-2}$$

was adopted.

The semi-direct models give good descriptions of the observed shape of the high-energy part of the gamma-ray spectrum. The intensity to the neutron single-particle states is dominant, as predicted by the theory, and the proportions are roughly accounted for. No intensity is observed to the neutron-hole states, e.g. $i_{13/2}^{-1}$ at 1.63 MeV and $f_{7/2}^{-1}$ at 2.34 MeV, in agreement with theory. (The $\frac{5+}{2}$, $\frac{7+}{2}$ doublet, $p_{1/2} x\ (3^-)$, at 2.6 MeV is also weakly populated by comparison with the $g_{9/2}$ state; this may be concluded from comparison with the ^{209}Bi(n, γ) spectrum, Fig. 1. The $g_{9/2}$ strength in ^{210}Bi, split among 10 levels, is close to the ground state.)

Gamma transitions to the neutron states $s_{1/2}$ at 4.6 MeV, $d_{3/2}$ at 5.1 MeV and $g_{7/2}$ at 5.2 MeV were not included in the semi-direct spectrum. The transition energies to these states are far below the peak of the giant resonance and the present calculations show that the direct capture cross sections are higher than the semi-direct cross sections.

The line structure of the gamma-ray spectrum weakens with decreasing neutron energy (see Fig. 3) at about the same rate as the expected semi-direct capture cross sections decrease. It seems likely that compound-nucleus processes give a significant contribution to the spectrum for $E_n \lesssim 6$ MeV.

While the semi-direct capture theory describes the shape of the spectrum well, the theoretical cross sections are much lower than those observed. Fig. 5 shows the cross section for neutron capture to the $p_{1/2}$, $(f_{5/2}^{-1} + p_{3/2}^{-1})$ and $g_{9/2}$ neutron states. In the theory of Brown[1)] both direct capture and interference between direct and semi-direct capture are included. The interference is constructive at the peak of the giant resonance and destructive below it. This gives cross section curves which are steeper than those based on the theory of Clement et al.[2], in which neither direct capture nor interference is taken into account.

The theories predict peak cross sections about $\frac{1}{10}$ of the experimental value for $p_{1/2}$ and about $\frac{1}{4}$ for $g_{9/2}$. For $(f_{5/2}{}^{-1} + p_{3/2}{}^{-1})$ the theories differ by a factor of 4 at the peak of the cross sections; the theory of Brown[1] gives a cross section $\frac{1}{5}$ of the experimental value and Clement et al.[2] $\frac{1}{20}$. The observed neutron energy dependence of the cross section to the $g_{9/2}$ state is in agreement with the theoretical predictions. The peak of this cross section curve is expected at $E_n = 9.7$ MeV, which is outside the range of the present experiment. The measured cross sections for $p_{1/2}$ and $(f_{5/2}{}^{-1} + p_{3/2}{}^{-1})$ decrease with increasing neutron energy. This dependence indicates a strong contribution of compound-nucleus processes. However, the shape of the gamma-ray spectrum (Figs. 3 and 4) shows that this contribution cannot be dominant for $E_n > 6$ MeV.

In conclusion, the shape of the gamma-ray spectra from $^{206}Pb(n, \gamma)$, $E_n \approx 8$ MeV, is found to be well described by the semi-direct capture theories. The theories give an enhancement of the direct capture cross section by a factor of 10-15 at the peak of the giant dipole resonance. The observed enhancement factor for $^{206}Pb(n, \gamma)$ is about 50.

REFERENCES

1. BROWN, G.E.,
Direct and semi-direct (p, γ) and (n, γ) reactions.
Nucl. Phys. 57 (1964) p. 339.

2. CLEMENT, C.F., LANE A.M. and ROOK J.R.,
Radiative capture by excitation of collective vibrations (I). Theory.
Nucl. Phys. 66 (1965) p. 273.

CLEMENT C.F., LANE A.M. and ROOK J.R.,
Radiative capture by excitation of collective vibrations (II). Calculation.
Nucl. Phys. 66 (1965) p. 293.

3. LUSHNIKOV A.A. and ZARETSKY D.F.,
Giant resonance in heavy nuclei.
Nucl. Phys. 66 (1965) p. 35.

4. DALY P.J. and SHAW P.F.D.,
Radiative proton capture cross-sections in heavy nuclei.
Nucl. Phys. 56 (1964) p. 322.

DALY P.J., ROOK J.R. and HODGSON P.E.,
Direct radiative proton capture reactions in cerium and bismuth.
Nucl. Phys. 56 (1964) p. 331.

5. CSIKAI J. et al.,
Radiative capture cross sections for 14.7 MeV neutrons.
Nucl. Phys. A95 (1967) p. 229.

6. MENLOVE H.O. et al.,
Neutron radiative capture cross sections for ^{23}Na, ^{55}Mn, ^{115}In and ^{165}Ho in the energy range 1.0 to 19.4 MeV.
Phys. Rev. 163 (1967) p. 1299.

7. CVELBAR, F. et al.,
Gamma-ray spectrum from the radiative capture of 14 MeV neutrons in ^{27}Al.
Phys. Letters 3 (1963) p. 364.

8. CVELBAR, F. et al.,
Radiative neutron capture in the region of the dipole giant resonance (I). Experiment.
Nucl. Phys. A130 (1969) p. 401.

CVELBAR, F. et al.,
Radiative capture of neutrons in the region of the dipole giant resonance (II). Calculations.
Nucl. Phys. A130 (1969) p. 413.

9. CVELBAR, F., HUDOKLIN, A. and POTOKAR, M.,
Gamma-ray spectra from the radiative capture of 14.1 MeV neutrons in Mg, Si, P and Ca.
Nucl. Phys. A138 (1969) p. 412.

10. DINTER, H.,
Gammaspektren und Wirkungsquerschnitte beim Einfang von 14 MeV Neutronen in ^{27}Al und ^{127}I.
Nucl. Phys. A111 (1968) p. 360.

11. BERGQVIST, I. et al.,
Gamma-ray spectra from the radiative capture of 7.4 MeV neutrons.
Phys. Letters 19 (1966) p. 670.

12. BERGQVIST, I. et al.,
Radiative capture in nickel and bismuth of neutrons in the MeV region.
Nucl. Phys. A120 (1968) p. 161.

13. BERGQVIST, I., LUNDBERG, B. and NILSSON, L.,
High-energy gamma-ray transitions from MeV neutron capture in ^{206}Pb.
Neutron Capture Gamma-Ray Spectroscopy. Int. symp. Studsvik, 11-15 Aug. 1969, (IAEA) Vienna, 1969 p. 569.

14. HALPERN, I.,
Private communication.

15. BAME, JR., S. J. et al.,
Absolute determination of monoenergetic neutron flux in the energy range 1 to 30 MeV.
Rev. Sci. Instr. 28 (1957) p. 997.

BAME, JR., S. J. et al.,
Counter telescope measurement of neutron flux.
Rev. Sci. Instr. 31 (1960) p. 911.

16. HALL, H. E. and BONNER, T. W.,
Gamma radiations from inelastic scattering of fast neutrons in ^{12}C, ^{14}N and ^{16}O.
Nucl. Phys. 14 (1959/60) p. 295.

17. CONDÉ, H. et al.,
Pulsed fast neutron research at the Los Alamos van de Graaff accelerator.
Nucl. Data for Reactors. Proc. of a conf., Paris 17-21 Oct. 1966, (IAEA) Vienna, 1967, Vol. 1, p. 419.

18. ROSEN, L. et al.,
Elastic scattering of 10.5- and 14.5-MeV polarized protons from nuclei and the optical model potential at intermediate energies.
Annals of Physics 34 (1965) p. 96.

19. RICHARD, P. et al.,
Two-neutron-hole configurations in ^{206}Pb from isobaric analog measurements.
Phys. Rev. 171 (1968) p. 1308.

20. LANE, A. M.,
Theory of radiative capture reactions.
Nucl. Phys. 11 (1959) p. 625.

LANE, A. M. and LYNN J.E.,
Analysis of experimental data on nucleon capture reactions.
Nucl. Phys. 11 (1959) p. 646.

FIGURE CAPTIONS

Fig. 1. Experimental gamma-ray spectra from $^{206}Pb(n,\gamma)$ and ^{209}Bi (n,γ) at 7.46 MeV, normalized to the same integrated neutron flux. The insert figure shows the time spectrum illustrating the sample (n,γ) peak and the background groups. Pulse heights corresponding to gamma transitions from the capturing state to levels below 3.0 MeV in ^{207}Pb and below 0.6 MeV in ^{210}Bi are indicated by vertical bars and the neutron single-particle configurations.

Fig. 2. Gamma-ray spectrum from the $^{12}C(n,\gamma)^{13}C$ reaction at 8.50 MeV. The solid curve represents the response line of the NaI(Tl) scintillator at 12.77 MeV. Transitions to the first excited state at 3.09 MeV and higher excited levels in ^{13}C give contributions at $\varepsilon_{\gamma} < 10$ MeV.

Fig. 3. Experimental gamma-ray spectra from the $^{206}Pb(n,\gamma)^{207}Pb$ reaction at various neutron energies. The spectra are plotted as functions of the residual excitation energy in ^{207}Pb. The spectra are normalized to the same integrated neutron flux. The solid and dashed curves show the unfolding of the spectra.

Fig. 4. Comparison between experimental and theoretical spectra at 7.46 MeV. The solid and dashed curves represent the spectra calculated from the semi-direct theories of Brown[1)] and Clement et al.[2)], respectively. The positions of the neutron single-particle states considered in the calculations are indicated. The spectra are normalized to each other in the excitation energy interval 2.5 - 3.5 MeV.

Fig. 5. Cross sections for the $^{206}Pb(n, \gamma)^{207}Pb$ reaction. The results from the first series of measurements are denoted by open triangles and from the second series by full dots. The solid and dashed curves are based on the semi-direct capture theories of Brown[1)] and Clement et al.[2)], respectively. The dot-dashed curve is the calculated direct capture cross section[20)]. Only an upper limit of the cross section for $g_{9/2}$ at 5.38 MeV was determined as indicated by the arrow.

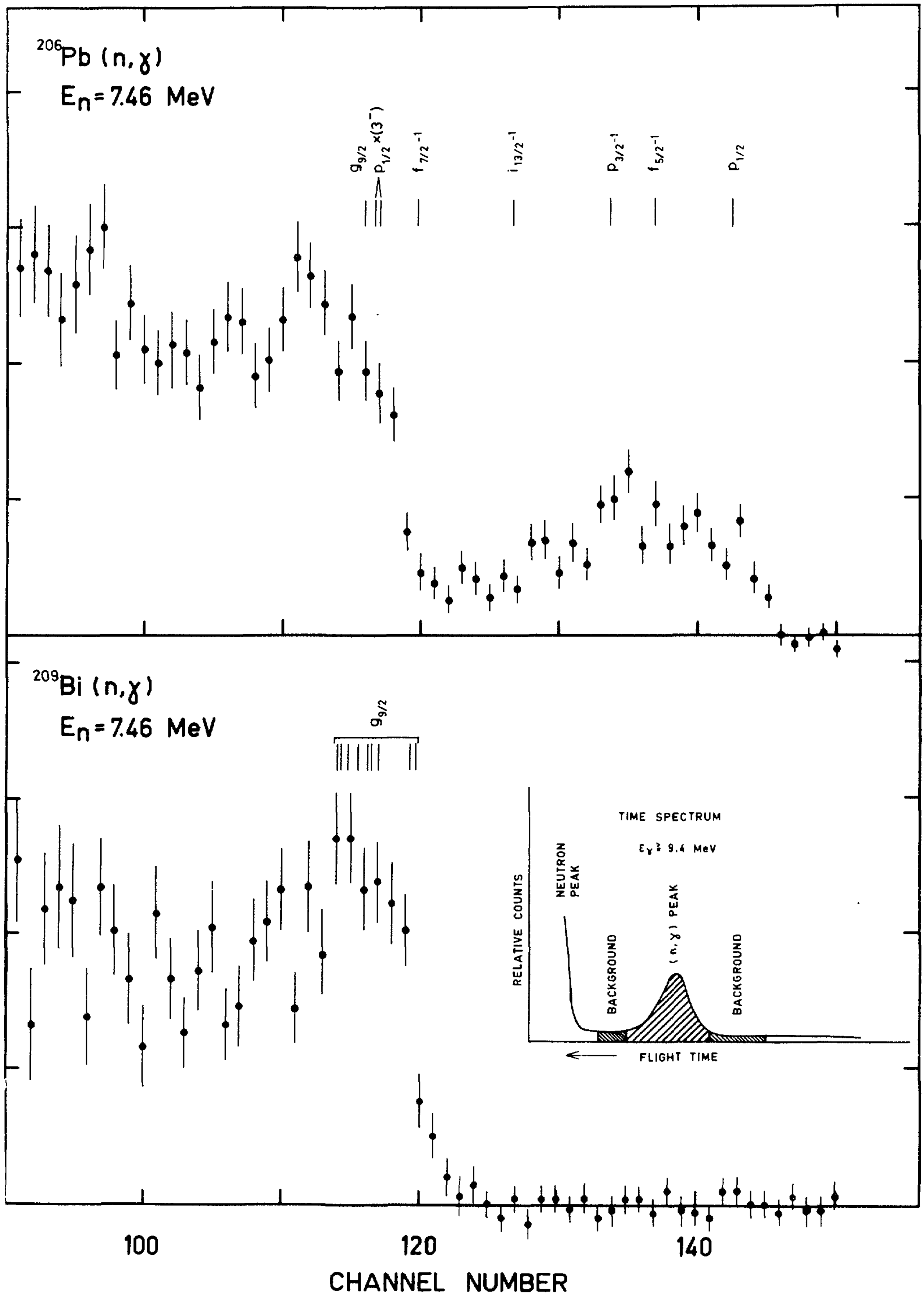

206Pb (n,γ)
En=7.46 MeV
g9/2
p1/2×(3−)
f7/2-1
i13/2-1
p3/2-1
f5/2-1
p1/2
209Bi (n,γ)
En=7.46 MeV
g9/2
TIME SPECTRUM
Eγ ≳ 9.4 MeV
RELATIVE COUNTS
NEUTRON PEAK
BACKGROUND
(n,γ) PEAK
BACKGROUND
FLIGHT TIME
100
120
140
CHANNEL NUMBER

Fig. 1.

Fig. 2.

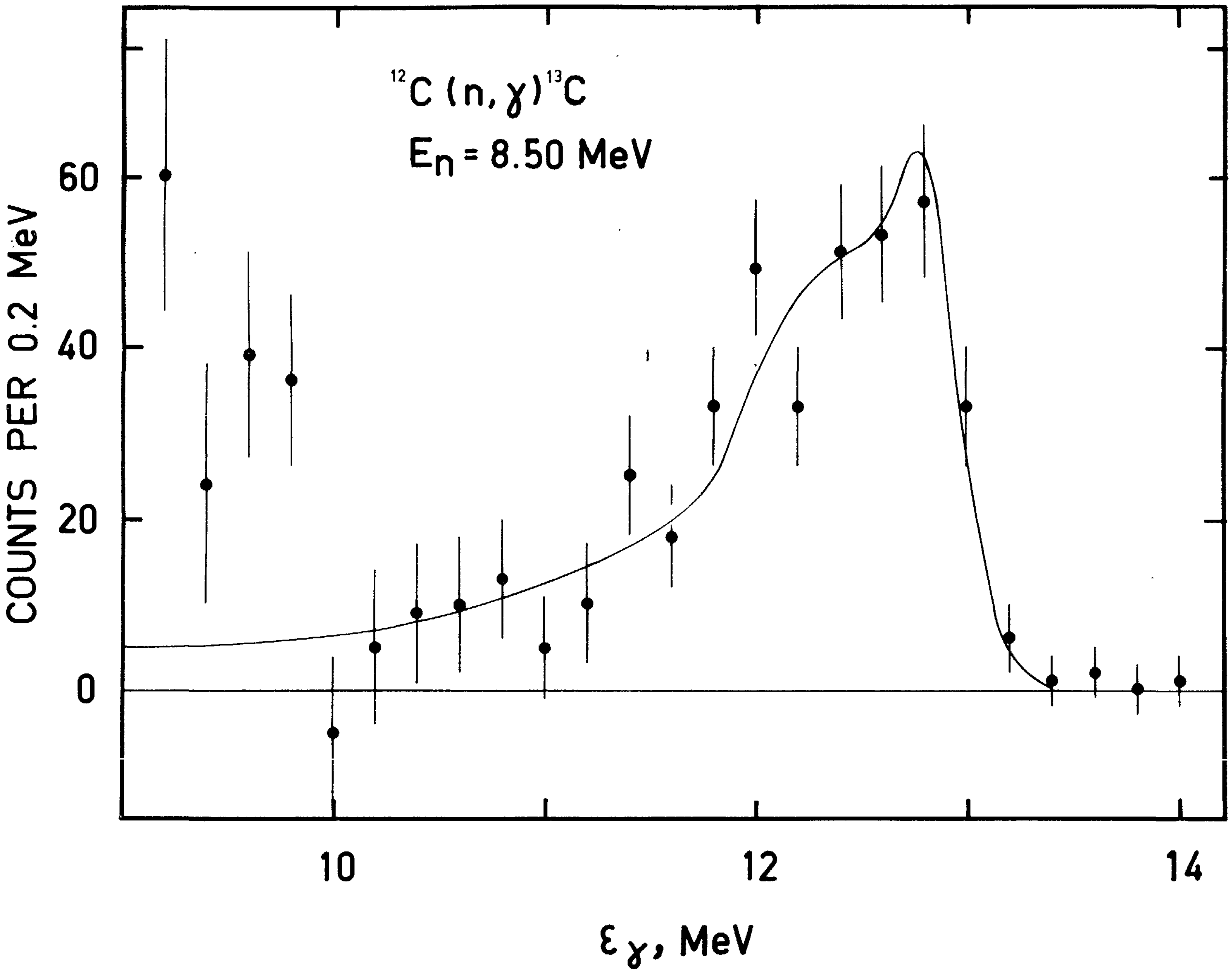

$^{12}C(n,\gamma)^{13}C$
$E_n = 8.50$ MeV
COUNTS PER 0.2 MeV
0
20
40
60
10
12
14
ε_γ, MeV

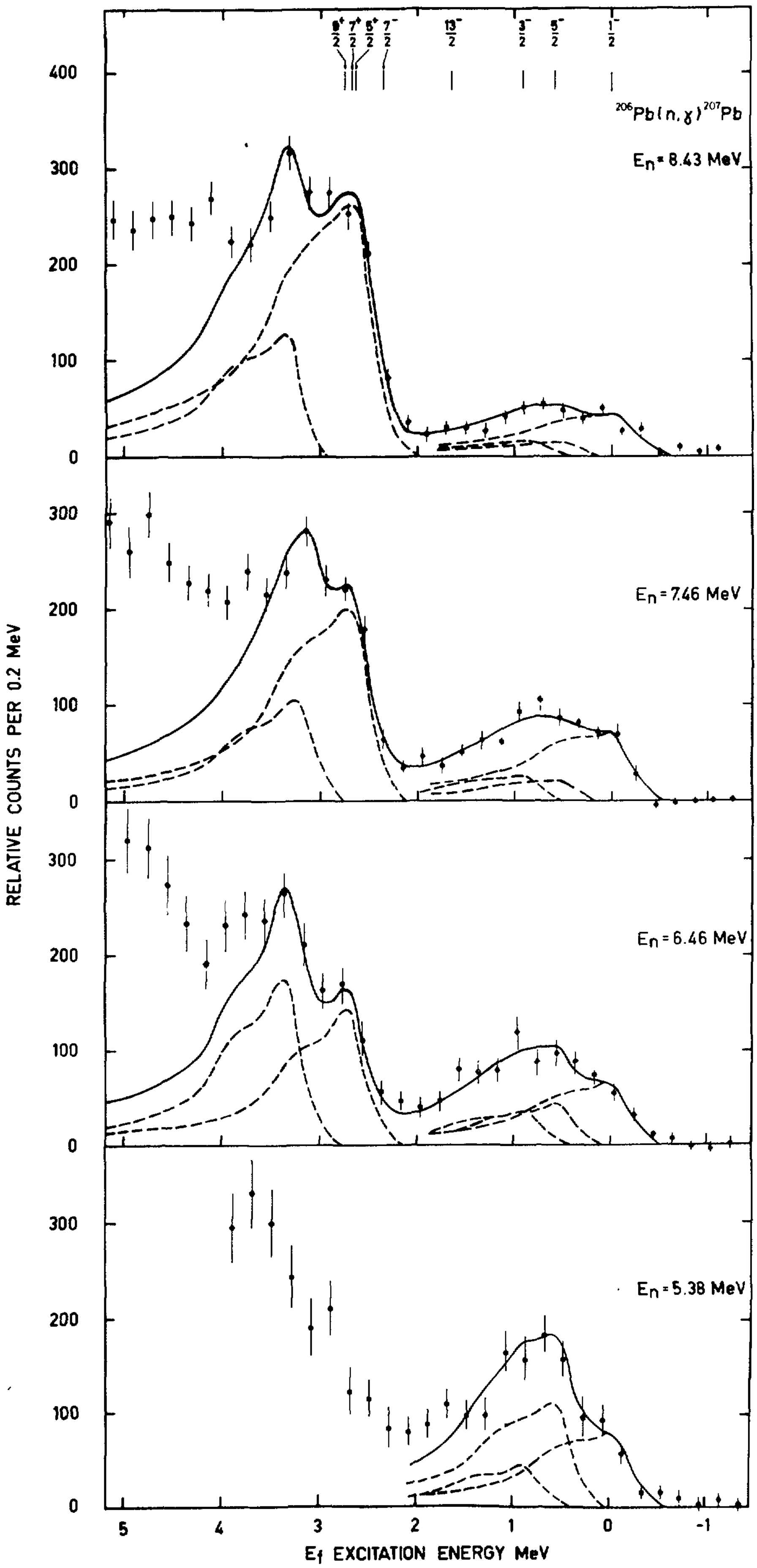

RELATIVE COUNTS PER 0.2 MeV
$^{206}Pb(n,\gamma)^{207}Pb$
E_n = 8.43 MeV
E_n = 7.46 MeV
E_n = 6.46 MeV
E_n = 5.38 MeV
$\frac{9}{2}^+$ $\frac{7}{2}^+$ $\frac{5}{2}^+$ $\frac{7}{2}^-$ $\frac{13}{2}^-$ $\frac{3}{2}^-$ $\frac{5}{2}^-$ $\frac{1}{2}^-$
E_f EXCITATION ENERGY MeV

Fig. 3.

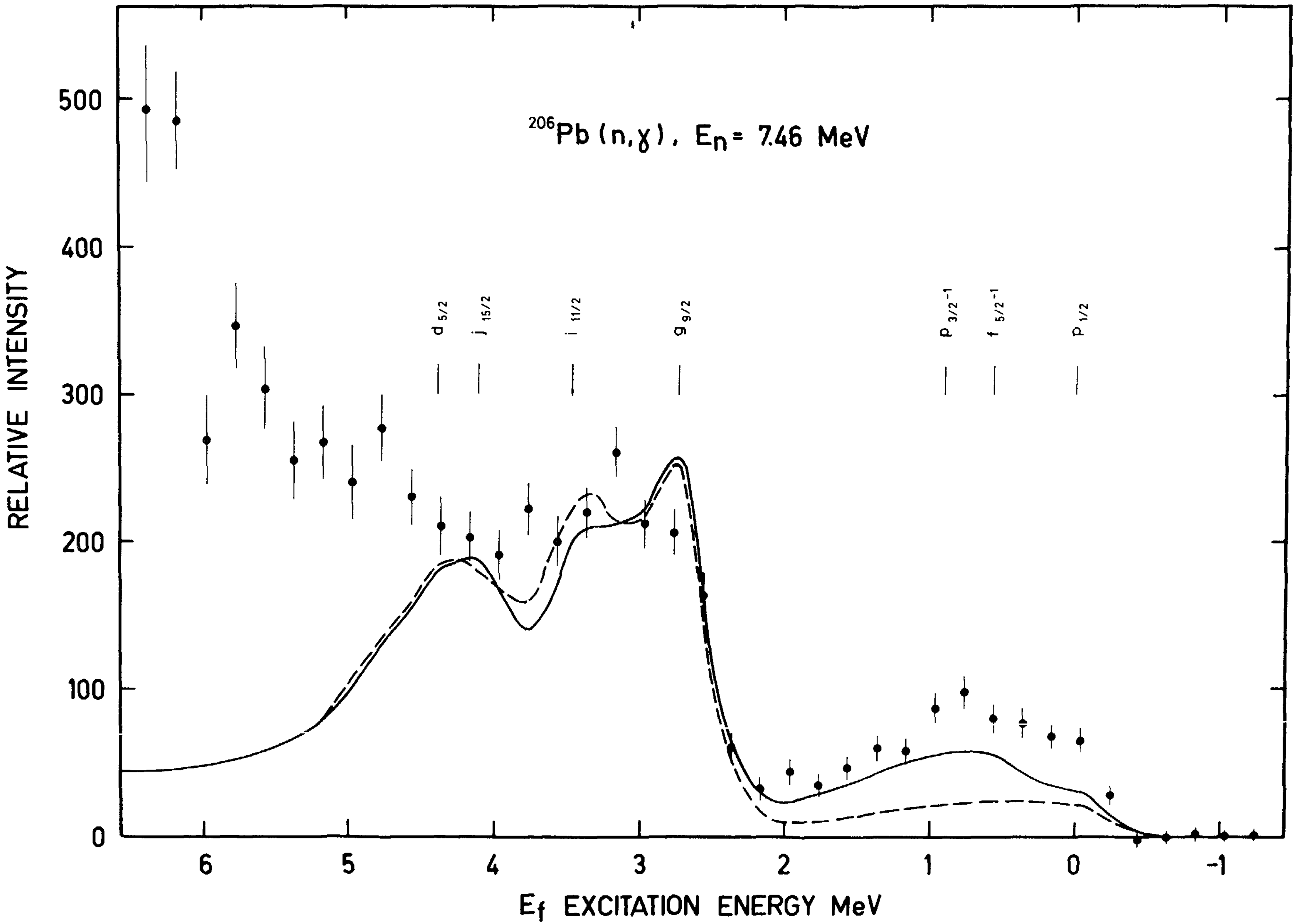
$^{206}Pb(n,\gamma)$, E_n = 7.46 MeV
RELATIVE INTENSITY
500
400
300
200
100
0
$d_{5/2}$
$j_{15/2}$
$i_{11/2}$
$g_{9/2}$
$p_{3/2}^{-1}$
$f_{5/2}^{-1}$
$p_{1/2}$
6
5
4
3
2
1
0
-1
E_f EXCITATION ENERGY MeV

Fig. 4.

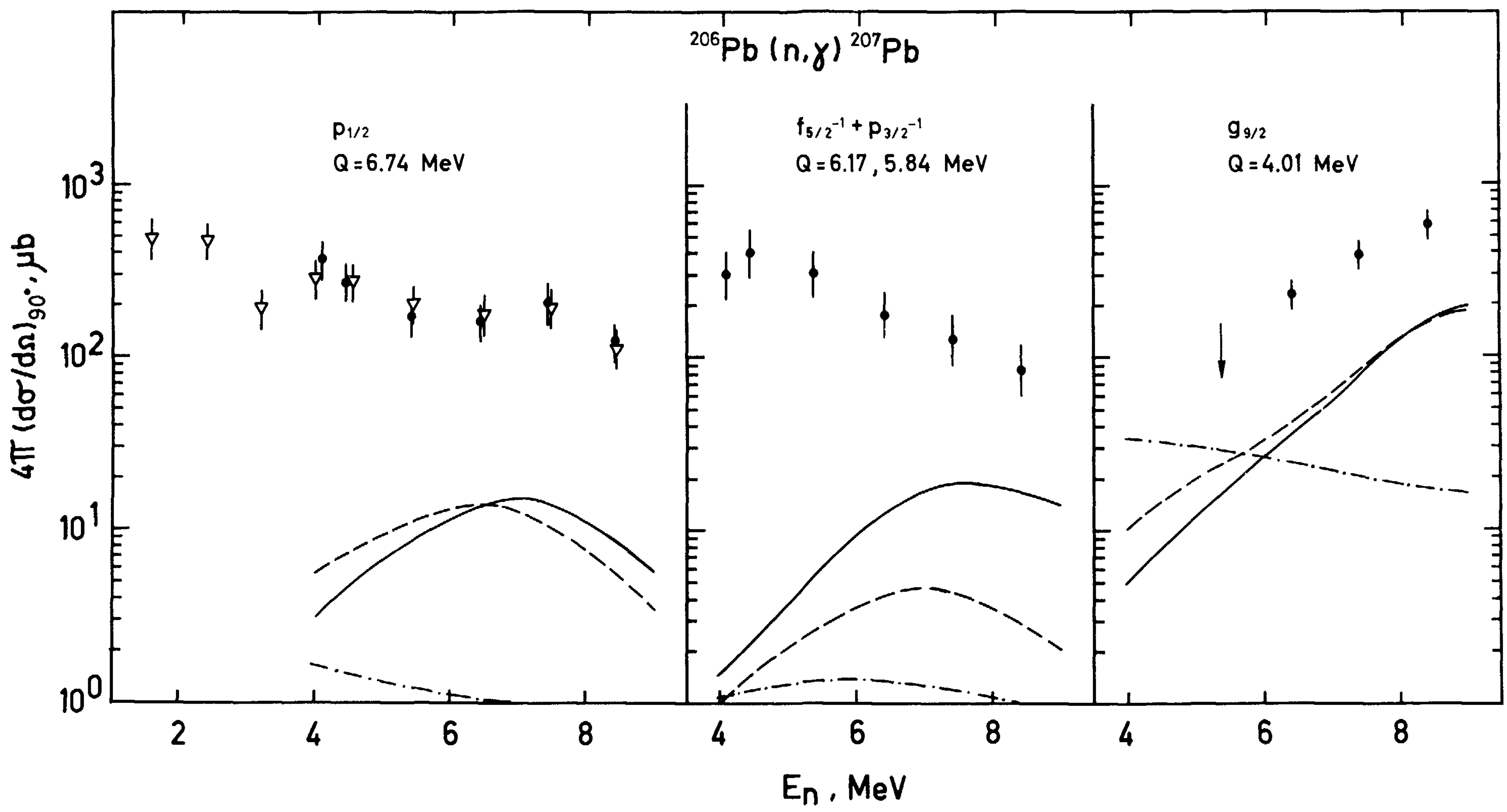

^{206}Pb (n,γ) ^{207}Pb
$p_{1/2}$
Q = 6.74 MeV
$f_{5/2}^{-1} + p_{3/2}^{-1}$
Q = 6.17, 5.84 MeV
$g_{9/2}$
Q = 4.01 MeV
$4\pi (d\sigma/d\Omega)_{90°}$, μb
10^0
10^1
10^2
10^3
2
4
6
8
E_n, MeV

Fig. 5.

LIST OF PUBLISHED AE-REPORTS

1–310 (See the back cover earlier reports.)

311. Spectroscopic study of recombination in the early afterglow of a helium plasma. By J. Stevefelt. 1968. 49 p. Sw. cr. 10:–.
312. Report on the personnel dosimetry at AB Atomenergi during 1966. By J. Carlsson and T. Wahlberg. 1968. 10 p. Sw. cr. 10:–.
313. The electron temperature of a partially ionized gas in an electric field. By F. Robben. 1968. 16 p. Sw. cr. 10:–.
314. Activation Doppler measurements on U238 and U235 in some fast reactor spectra. By L. I. Tirén and I. Gustafsson. 1968. 40 p. Sw. cr. 10:–.
315. Transient temperature distribution in a reactor core with cylindrical fuel rods and compressible coolant. By H. Vollmer. 1968. 38 p. Sw. cr. 10:–.
316. Linear dynamics model for steam cooled fast power reactors. By H. Vollmer. 1968. 40 p. Sw. cr. 10:–.
317. A low level radioactivity monitor for aqueous waste. By E. J. M. Quirk. 1968. 35 p. Sw. cr. 10:–.
318. A study of the temperature distribution in UO_2 reactor fuel elements. By I. Devold. 1968. 82 p. Sw. cr. 10:–.
319. An on-line water monitor for low level β-radioactivity measurements. By E. J. M. Quirk. 1968. 26 p. Sw. cr. 10:–.
320. Special cryostats for lithium compensated germanium detectors. By A. Lauber, B. Malmsten and B. Rosencrantz. 1968. 14 p. Sw. cr. 10:–.
321. Stability of a steam cooled fast power reactor, its transients due to moderate perturbations and accidents. By H. Vollmer. 1968. 36 p. Sw. cr. 10:–.
322. Progress report 1967. Nuclear chemistry. 1968. 30 p. Sw. cr. 10:–.
323. Noise in the measurement of light with photomultipliers. By F. Robben. 1968. 74 p. Sw. cr. 10:–.
324. Theoretical investigation of an electrogasdynamic generator. By S. Palmgren. 1968. 36 p. Sw. cr. 10:–.
325. Some comparisons of measured and predicted primary radiation levels in the Ågesta power plant. By E. Aalto, R Sandlin and A. Krell. 1968. 44 p. Sw. cr. 10:–.
326. An investigation of an irradiated fuel pin by measurement of the production of fast neutrons in a thermal column and by pile oscillation technique. By Veine Gustavsson. 1968 24 p. Sw. cr. 10:–.
327. Phytoplankton from Tvären, a bay of the Baltic, 1961–1963. By Torbjörn Willén. 1968. 76 p. Sw. 10:–.
328. Electronic contributions to the phonon damping in metals. By Rune Jonson. 1968. 38 p. Sw. cr. 10:–.
329. Calculation of resonance interaction effects using a rational approximation to the symmetric resonance line shape function. By H. Häggblom. 1968. 48 p. Sw. cr 10:–.
330. Studies of the effect of heavy water in the fast reactor FR0. By L. I. Tirén, R. Håkansson and B. Karmhag. 1968. 26 p. Sw. cr. 10:–.
331. A comparison of theoretical and experimental values of the activation Doppler effect in some fast reactor spectra. By H. Häggblom and L. I. Tirén. 1968. 28 p. Sw. cr. 10:–.
332. Aspects of low temperature irradiation in neutron activation analysis. By D Brune. 1968. 12 p. Sw. cr. 10:–.
333. Application of a betatron in photonuclear activation analysis. By D. Brune, S. Mattsson and K. Lidén. 1968. 13 p. Sw. cr. 10:–.
334. Computation of resonance-screened cross section by the Dorix-Speng system. By H. Häggblom. 1968. 34 p. Sw. cr. 10:–.
335. Solution of large systems of linear equations in the presence of errors. A constructive criticism of the least squares method. By K. Nygaard. 1968. 28 p. Sw. cr. 10:–.
336. Calculation of void volume fraction in the subcooled and quality boiling regions. By S. Z. Rouhani and E. Axelsson. 1968. 26 p. Sw. cr. 10:–.
337. Neutron elastic scattering cross sections of iron and zinc in the energy region 2.5 to 8.1 MeV. By B. Holmqvist, S. G. Johansson, A. Kiss, G. Lodin and T. Wiedling. 1968. 30 p. Sw. cr. 10:–.
338. Calibration experiments with a DISA hot-wire anemometer. By B. Kjellström and S. Hedberg. 1968. 112 p. Sw. cr. 10:–.
339. Silicon diode dosimeter for fast neutrons. By L. Svansson, P. Swedberg, C-O. Widell and M. Wik. 1968. 42 p. Sw. cr. 10:–.
340. Phase diagrams of some sodium and potassium salts in light and heavy water. By K. E. Holmberg. 1968 48 p. Sw. cr. 10:–.
341. Nonlinear dynamic model of power plants with single-phase coolant reactors. By H. Vollmer. 1968. 26 p. Sw. cr. 10:–.
342. Report on the personnel dosimetry at AB Atomenergi during 1967. By J. Carlsson and T. Wahlberg. 1968. 10 p. Sw. cr. 10:–.
343. Friction factors in rough rod bundles estimated from experiments in partially rough annuli – effects of dissimilarities in the shear stress and turbulence distributions. By B. Kjellström. 1968. 22 p. Sw. cr. 10:–.
344. A study of the resonance interaction effect between ^{238}U and ^{239}Pu in the lower energy region. By H. Häggblom. 1968. 48 p. Sw. cr. 10:–.
345. Application of the microwave discharge modification of the Wilzbach technique for the tritium labelling of some organics of biological interest. By T. Gosztonyi. 1968. 12 p. Sw. cr. 10:–.
346. A comparison between effective cross section calculations using the intermediate resonance approximation and more exact methods. By H. Häggblom. 1969. 64 p. Sw. cr. 10:–.
347. A parameter study of large fast reactor nuclear explosion accidents. By J. R. Wiesel. 1969. 34 p. Sw. cr. 10:–.
348. Computer program for inelastic neutron scattering by an anharmonic crystal. By L. Bohlin, I. Ebbsjö and T. Högberg. 1969. 52 p. Sw. cr. 10:–.
349. On low energy levels in ^{185}W. By S. G. Malmskog, M. Höjeberg and V. Berg. 1969. 18 p. Sw. cr. 10:–.
350. Formation of negative metal ions in a field-free plasma. By E. Larsson. 1969. 32 p. Sw. cr. 10:–.
351. A determination of the 2 200 m/s absorption cross section and resonance integral of arsenic by pile oscillator technique. By E. K. Sokolowski and R. Bladh. 1969. 14 p. Sw. cr. 10:–.
352. The decay of ^{191}Os. By S. G. Malmskog and A. Bäcklin. 1969. 24 p. Sw. cr. 10:–.
353. Diffusion from a ground level point source experiment with thermoluminescence dosimeters and Kr 85 as tracer substance. By Ch. Gyllander, S. Hollman and U. Widemo. 1969. 23 p. Sw. cr. 10:–.
354. Progress report, FFN, october 1, 1967 – september 30, 1968. By T. Wiedling. 1969. 35 p. Sw. cr. 10:–.
355. Thermodynamic analysis of a supercritical mercury power cycle. By A. S. Roberts, Jr., 1969. 25 p. Sw. cr. 10:–.
356. On the theory of compensation in lithium drifted semiconductor detectors. By A. Lauber. 1969. 45 p. Sw. cr. 10:–.
357. Half-life measurements of levels in ^{75}As. By M. Höjeberg and S. G. Malmskog. 1969. 14 p. Sw. cr. 10:–.
358. A non-linear digital computer model requiring short computation time for studies concerning the hydrodynamics of the BWR. By F. Reisch and G. Vayssier. 1969. 38 p. Sw. cr. 10: –.
359. Vanadium beta emission detectors for reactor in-core neutron monitoring. I. Ö. Andersson and B. Söderlund. 1969. 26 p. Sw. cr. 10:–.
360. Progress report 1968 nuclear chemistry. 1969. 38 p. Sw. cr. 10:–.
361. A half-life measurement of the 343.4 keV level in ^{175}Lu. By M. Höjeberg and S. G. Malmskog. 1969. 10 p. Sw. cr. 10:–.
362. The application of thermoluminescence dosimeters to studies of released activity distributions. By B-I. Rudén. 1969. 36 p. Sw. cr. 10:–.
363. Transition rates in ^{161}Dy. By V. Berg and S. G. Malmskog. 1969. 32 p. Sw. cr 10:–.
364. Control rod reactivity measurements in the Ågesta reactor with the pulsed neutron method. By K. Björeus. 1969. 44 p. Sw. cr. 10:–.
365. On phonons in simple metals II. Calculated dispersion curves in aluminium. By R. Johnson and A. Westin. 1969. 124 p. Sw. cr. 10:–.
366. Neutron elastic scattering cross sections. Experimental data and optical model cross section calculations. A compilation of neutron data from the Studsvik neutron physics laboratory. By B. Holmqvist and T. Wiedling. 1969. 212 p. Sw. cr 10:–.
367. Gamma radiation from fission fragments. Experimental apparatus – mass spectrum resolution. By J. Higbie. 1969. 50 p. Sw. cr. 10:–.
368. Scandinavian radiation chemistry meeting Studsvik and Stockholm, september 17–19, 1969. By H. Christensen. 1969. 34 p. Sw. cr. 10:–.
369. Report on the personnel dosimetry at AB Atomenergi during 1968. By J. Carlsson and T. Wahlberg. 1969. 10 p. Sw. cr 10:–.
370. Absolute transition rates in ^{188}Ir. By S. G. Malmskog and V. Berg. 1969. 16 p. Sw. cr. 10:–.
371. Transition probabilities in the 1/2+(631) Band in ^{235}U. By M. Höjeberg and S. G. Malmskog. 1969. 18 p. Sw. cr. 10:–.
372. E2 and M1 transition probabilities in odd mass Hg nuclei. By V. Berg, A. Bäcklin, B. Fogelberg and S. G. Malmskog. 1969. 19 p. Sw. cr. 10:–.
373. An experimental study of the accuracy of compensation in lithium drifted germanium detectors. By A. Lauber and B. Malmsten. 1969. 25 p. Sw. cr. 10:–.
374. Gamma radiation from fission fragments. By J. Higbie. 1969. 22 p. Sw. cr. 10:–.
375. Fast Neutron Elastic and Inelastic Scattering of Vanadium. By B. Holmqvist, S. G. Johansson, G. Lodin and T. Wiedling. 1969. 48 p. Sw. cr. 10:–.
376. Experimental and Theoretical Dynamic Study of the Ågesta Nuclear Power Station. By P.-Å. Bliselius, H. Vollmer and F. Åkerhielm. 1969. 39 p. Sw. cr. 10: –
377. Studies of Redox Equilibria at Elevated Temperatures 1. The Estimation of Equilibrium Constants and Standard Potentials for Aqueous Systems up to 374°C. By Derek Lewis. Sw. cr. 10:-
378. The Whole Body Monitor HUGO II at Studsvik. Design and Operation. By L. Devell, I. Nilsson and L. Venner. 1970. 26 p. Sw. cr. 10:-.
379. ATOMSPHERIC DIFFUSION Investigations at Studsvik and Ågesta 1960–1963. By L-E Hæggblom, Ch Gyllander and U Widemo. 1969. 91 p. Sw. cr. 10: –
380. An expansion method to unfold proton recoil spectra. By J. Kockum. 1970. 20 p. Sw. cr. 10: –.
381. The 93.54 keV level in ^{91}Sr, and evidence for 3-neutron states above N=50. By S. G. Malmskog and J. Mc Donald. 1970. 24 p. Sw. cr. 10:-.
382. The low energy level structure of ^{191}Ir. By S. G. Malmskog, V. Berg, A. Bäcklin and G. Hedin. 1970. 24 p. Sw. cr. 10:–.
383. The drinking rate of fish in the Skagerack and the Baltic. J. E. Larsson. 16 p. Sw. cr. 10: –.
384. Lattice dynamics of NaCl, KCl, RbCl and RbF. G. Raunio and S. Rolandson 26 p. Sw. cr. 10: –.
385. A neutron elastic scattering study of chromium, iron and nickel in the energy region 1.77 to 2.76 MeV. 26 p. By B. Holmqvist, S .G Johansson, G. Lodin, M. Salama and T. Wiedling. 1970. Sw. cr. 10: –
386. The decay of bound isobaric analogue states in ^{28}Si and ^{32}S using (d, nγ) reactions. By L. Nilsson, A. Nilsson and I. Bergqvist. 1970. 34 p. Sw. cr. 10:–.
387. Transition probabilities in ^{189}Os. By S. G. Malmskog, V. Berg and A. Bäcklin. 1970. 40 p. Sw. cr. 10: –.
388. Cross sections for high-energy gamma transitions from MeV neutron capture in ^{206}Pb. By I. Bergqvist, B. Lundberg and L. Nilsson. 1970. 16 p. Sw. cr. 10: –.

List of published AES-reports (In Swedish)

1. Analysis be means of gamma spectrometry. By D. Brune. 1961. 10 p. Sw. cr. 6:–.
2. Irradiation changes and neutron atmosphere in reactor pressure vessels-some points of view. By M. Grounes. 1962. 33 p. Sw. cr. 6:–.
3. Study of the elongation limit in mild steel. By G. Östberg and R. Attermo. 1963 17 p. Sw. cr. 6:–.
4. Technical purchasing in the reactor field. By Erik Jonson. 1963. 64 p. Sw. cr. 8:–.
5. Ågesta nuclear power station. Summary of technical data, descriptions, etc. for the reactor. By B. Lilliehöök. 1964. 336 p. Sw. cr. 15:–.
6. Atom Day 1965. Summary of lectures and discussions. By S. Sandström. 1966. 321 p. Sw. cr. 15:–.
7. Building materials containing radium considered from the radiation protection point of view. By Stig O. W. Bergström and Tor Wahlberg. 1967. 26 p. Sw. cr. 10:–.

Additional copies available from the library of AB Atomenergi, Fack, S-611 01 Nyköping, Sweden.

EOS-tryckerierna, Stockholm 1970